International Journal of GEOMATE, May, 2025 Vol.28, Issue 129, pp.105-112
ISSN: 2186-2982 (P), 2186-2990 (O), Japan, DOI: https://doi.org/10.21660/2025.129.g14225
Geotechnique, Construction Materials and Environment

LAND SUBSIDENCE ANALYSIS IN PALEMBANG CITY USING DIFFERENTIAL INTERFEROMETRIC SAR

Sri Rezki Artini[1], *Rosidawani[2] and Dinar Dwi Anugerah Putranto[3]

[1]Doctoral Program in Engineering, Postgraduate Program, Faculty of Engineering, Universitas Sriwijaya
[2,3]Department of Civil Engineering and Planning, Faculty of Engineering, Universitas Sriwijaya, Indonesia

*Corresponding Author, Received: 18 Jan. 2025, Revised: 10 Feb. 2025, Accepted: 13 Feb. 2025

ABSTRACT: Palembang is a city that has expanded from the banks of the Musi River to the surrounding plains, including river deltas and reclaimed swampy regions, increasing the risk of land subsidence, particularly in low-lying areas. Continuous changes in subsurface conditions have led to excessive land deformation, posing risks to buildings, underground infrastructure, and overall human safety. Recently, land subsidence in Palembang has become a growing concern due to its impact on infrastructure development and worsening waterlogging caused by rising sea levels encroaching on the mainland. This study employs Synthetic Aperture Radar (SAR) imagery and the Differential Interferometric SAR (D-InSAR) method to map areas of subsidence and uplift in Palembang. As of August 2024, subsidence values in the city range from -14 cm to -51.4 cm, with the Swamp Deposit (Qs) area being the most affected. Geological analysis indicates that subsidence is influenced by population growth, urban infrastructure expansion, increasing building floor area, and the presence of the reservoir-bearing Airbenakat Formation. The most significant subsidence occurred in relatively young Quaternary deposits, likely due to compaction-induced settling. Compared to other Indonesian cities—Jakarta (-3 to -10 cm/year), Semarang (-6 to -8 cm/year), Surabaya (-6 to -10 cm/year), and Bandung (-7.6 to -23 cm/year)—Palembang exhibits a substantial rate of land subsidence. To mitigate this issue, a more adaptive spatial development strategy should be prioritized to reduce subsidence and ensure sustainable urban growth.

Keywords: D-InSAR, Land subsidence, Swamp deposit, Quarter

1. INTRODUCTION

Studies and explorations on the phenomenon of land subsidence in several countries are very interesting. There are various causes of land subsidence, which can be both natural and non-natural [1]. Specifically, natural land subsidence can be caused by several factors, such as geological processes and cycles. These factors include the activity of moving tectonic plates [2], natural compaction [3], volcanic activity, and the processes in geothermal areas [4], etc.

Meanwhile, non-natural land subsidence can occur due to anthropogenic activities, namely the withdrawal of fluids from the ground, such as extraction of water and oil through pumping [5], extraction of solid materials from the soil (mining activities) [6], and imposition of heavy loads on land (multi-story building structures and settlements) [7]. Generally, the magnitude of land subsidence varies across different areas, and the causes of this variation can also differ spatially and temporally [8].

Table 1 Stratigraphy of Palembang City

Period	Era		Period		Litostratigrafi	Formation	Lithology
K E N Z O I K U M	Quarter		Holosen		QS	Swamp, sediment/lake sediment	Lake sediment are composed of mud, sild and sand
			Plistosen				
			Pliosen				
	T E R S I E R	N E O G E N	Miosen	End	Tma Tertiary, Miosen, Air Benakat)	Air Benakat Formation	Air Benakat formation is composed of alternating mudstone, siltstone, and shale, which is generally calcareous and carbonate
				Middle			
					Tmg (Tertiary, Miosen, Gumai)	Gumai Formation	Gumai formation is composed of mudstone, shale, and in some
			Oligosen	Primary	Tomt(Tersier, Oligosen, Miosen, Talang Akar)	Talangakar Formation	Talangakar formation is composed of calcareous sandstone, quartz sandstone, intercalated by claystone shale, and thin layers of coal
				End			

1.1 Geological Conditions of The Study Area

Based on the stratigraphy of Palembang City shown in Table 1. The city comprises several geological formations, including one Quaternary formation known as Swamp/lake Deposits (Qs), two Tertiary-Miocene formations, which are Airbenakat Formation (Tma), and Gumai Formation (Tmg). In addition, the city also consists of one Tertiary-Oligocene-Miocene formation, namely Talangakar Formation (Tomt). These four formations are primarily composed of sedimentary rock lithology.

1.2 Land Subsidence

Reclamation projects along the road network towards the development of Tanjung Api-Api port and Special Economic Zone on the coast of South Sumatra Province have expanded areal development and continuously changed the subsurface conditions of unwanted land deformation [10]. Monitoring can be conducted through geodetic observations by installing several control points and performing regular observations over a certain period. Additionally, the development of technology has enabled the use of high-resolution radar imagery for land subsidence monitoring. When considering accuracy, the GNSS (Global Navigation Satellite System) method, which uses height difference measurements, is considered the most accurate for land subsidence detection [11,12]. Other methods that also have quite good accuracy in identifying areas prone to land subsidence are interferometric Synthetic Aperture Radar (InSAR) [13-15], and gravity technology [16].

2. RESEARCH SIGNIFICANCE

Land subsidence endangers lowland areas, causing infrastructure damage, structural instability, and increased flood risks. Without monitoring, waterlogging worsens due to poor drainage, and buildings deteriorate over time. This study emphasizes the need for continuous subsidence assessment to enhance urban resilience. By identifying vulnerable areas, policymakers can implement adaptive strategies, improve infrastructure, and mitigate risks, ensuring sustainable urban development and long-term safety for communities in Palembang.

3. METHODS

An analysis was conducted to examine land subsidence across different land use typologies at various observed locations using two methods. These methods included image interpretation with D-InSAR and observation with GNSS.

3.1 Study Sites

Palembang City is the capital of South Sumatra Province surrounded by watery land, as shown in Fig. 1, which comes from swamp puddles and the overflow of Musi River. Geographically, the city is located between 2° 59′ 27.99″ S to 3° 5’ S and between 104° 35′ 24.24″ to 104° 52’ 30” East Longitude. The topography is generally flat and hilly with the highest altitude being Siguntang Hill at 14 m above sea level. Moreover, the rest of the area is in the lowlands, with swamps along Musi River and tributaries with an average elevation of 2-4 m above sea level. Geologically, Palembang experiences low land movement, but the impact of land subsidence significantly affects infrastructure, subjecting buildings to cracks.

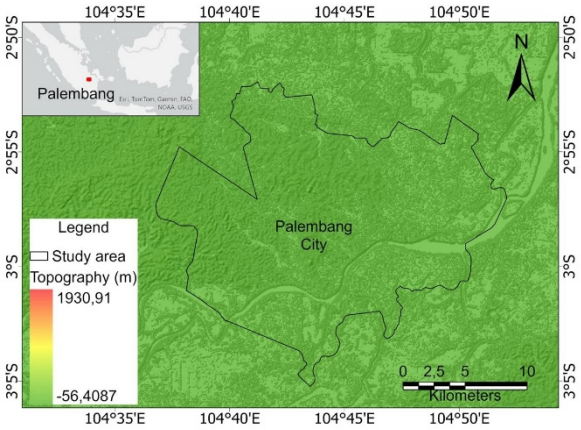

Fig. 1 Study Area, Palembang City

3.2 D-InSAR

SAR Image Extraction was performed in two stages which were InSAR and D-InSAR methods [17]. The stages included :(1) importing additional data and information;(2) image co-registration;(3) initial processing;(4) interferogram and calculating coherence;(5) interferogram filtration;(6) phase unwrapping;(7) absolute phase to height; and (8) absolute phase to displacement. The recording time of master and slave images in Figure 2 shows the result of surface movement [18].

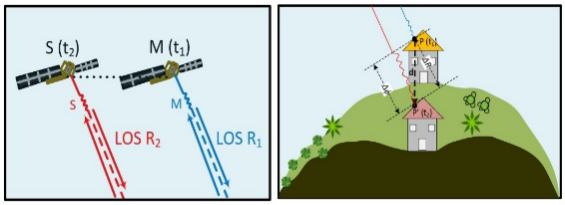

Fig.2 (a) When recording the master image and slave image; (b). phase difference as a result of the phenomenon of ground surface movement.

Therefore, the equation regarding the interferogram phase can be explained as shown in equation 1.

Interferogram phase equation, on master and slave images due to ground surface movement phenomena,

$$\Delta\emptyset = \emptyset\_(1) - \emptyset\_2$$
$$\Delta\emptyset = 4\pi/\lambda\ (R\_(1) + R\_2)$$
$$\Delta\emptyset = 4\pi/\lambda\ \Delta R \quad (1)$$

In equation (1), the phase difference of interferogram was denoted by $\Delta\emptyset$, wavelength was represented by λ, while the relative difference in Line of Sight (LoS) was indicated by ΔR. Based on the calculation, the difference in the position of the satellite observer on the same object could cause a difference in LoS. Similarly, the difference in LoS could be caused by changes in the position of the object on the Earth's surface recorded by the same satellite [19].

During SAR image processing, phase to displacement was a phase change from refinement and re-flattening into a LoS displacement value [20]. These displacement measurements typically ranged from fractions of millimeters to centimeters. After the refinement and re-flattening process (phase unwrapping results), two displacement conversion methods existed. The first method was phase to displacement, which was the process of changing the phase to vertical displacement in LoS and providing information in the form of LoS. The second method was phase to vertical displacement, and it comprised changing the phase difference into actual vertical displacement (true). While the first method produced LoS displacement, the second provided actual displacement information [21]. The calculation of the phase to vertical displacement (true) was performed using equation 2 [22].

$$Displacement\ vertical = \frac{\text{fase unwrapped} * 0.056}{-4\pi \cos\theta} \quad (2)$$

From equation 2, the angle formed between the wave beam and the perpendicular line to the surface of the object on the Earth's surface was denoted by θ (incidence angle). Information about the incidence angle was found in the metadata of each SAR image. In a situation where the SAR image processing already had a LoS displacement, then the vertical displacement could be obtained using the following equation 3

$$\text{Displacement vertical (true)} = \text{LoS}/(\cos\theta) \quad (3)$$

Equation 3 was the displacement LoSS, which was then compared with the cos incidence angle value without including other parameters from InSAR image.

In this study, the method flow diagrams shown in Fig. 3 were generally applicable, including SAR image with X, C, L, and P bands. The stages of importing additional data and information included reading data files and parameters from CEOS format, as well as processing parameter formation [23]. Additionally, image co-registration stages included searching for similar points in a pair of master and slave images, determining the transformation of the slave image to the master image, and determining the overlapping area [24].

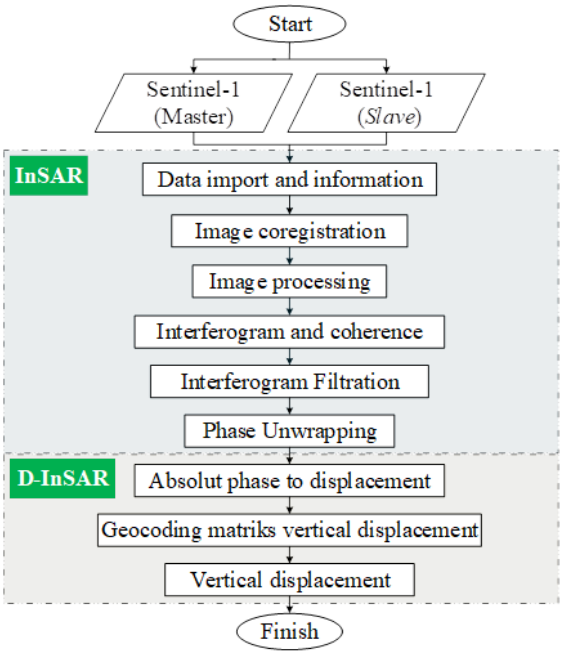

Fig. 3 InSAR and D-InSAR flow diagram

The data used in this study were SAR Sentinel-1A level 1 images from ESA (European Space Agency) downloaded from the Alaska website https://search.asf.alaska.edu/ for the period 2014 to 2023. SAR image had the characteristics of SLC (Single Look Complex) type of C-band sensor. Following this discussion, the selection of image pairs was an important stage in analyzing land surface deformation using D-InSAR method.

Table 2: Perpendicular baseline length and time interval of the image.

Master Image ID Scene	Slave Image ID Scene	Acquisition Time	Baseline perpendicular (m)	Time Interval (days)
Sentinel-1A October 29, 2014	Sentinel-1A August 28, 2019	December 9, 2023	-28	1764
Sentinel-1A August 28, 2019	Sentinel-1A August 28, 2024	October 9, 2024	3	1464

Table 2 showed the baseline length measured on two pairs of images consisting of two master images and slave images. The highest perpendicular baseline in the image pair was on August 28, 2019. However, the shortest time interval was in the paired image with the slave image on August 28, 2024.

3.3 Land Subsidence Monitoring Network Optimization Design

Horizontal control network observation was conducted using GNSS method based on control points that were installed according to the choice of locations representing landfills in swamp areas (swamp sediment), Air Benakat Formation, Talang Akar Formation, and Gumai Formation. In this exploration, new control points were installed, and existing points from 2004 were used as a basis for observing land subsidence at the selected area forming the control point network design at locations representing the four formations (Fig.4).

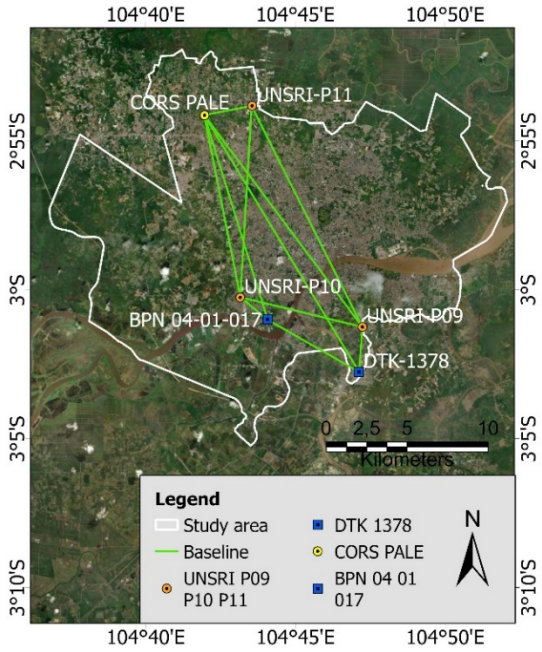

Fig. 4 Design of land subsidence monitoring control point network configuration with GNSS (2024).

4. RESULTS AND DISCUSSION

The master data used for Sentinel-1 imagery was from October 2014, while the slave data was collected in August 2019. Figure 5(a) showed VV (Vertical-Vertical) coherence for Palembang City in August 2019, with values ranging from coherence of 0.040 to 0.920 π. Following the discussion, the standard coherence value typically ranged from 0 to 1π. In 2023, VV coherence values were again between 0.040 to 0.920 π, as shown in Fig. 5(b) for August 2023.

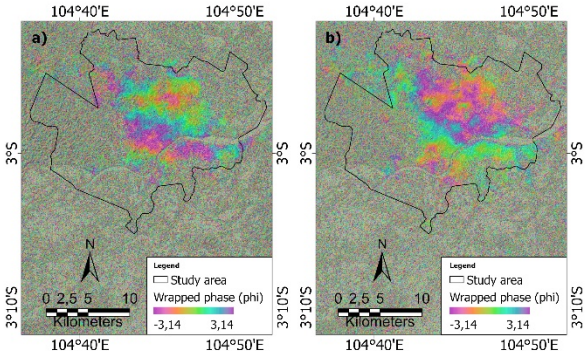

Fig. 5 Phase Interferogram; (a) August 2019-2023, (b) August 2014-2019

4.1 Phase Interferogram

Interferogram phase (VV phase) had a significant difference, showing land subsidence in Palembang City.

However, there was still some uncertainty in the phase due to being in the range of +2phi to -2phi. The interpretation of interferogram phase showed a change in the surface shape of the city.

Based on Fig. 5, VV phase value in both periods was -3.0 to 3.0 phi. This phase value varied due to dry or rainy season conditions in the study area. Additionally, differences in VV phase values were also caused by the type of data used or the quality of input data, affecting accuracy and precision.

4.2 Vertical Displacement Extraction For The August 2019 Period

In the displacement stage, three file integrations were used, namely coherence, unwrapped phase, and DEM. The phase-to-displacement stage used basic parameters which included product coherence threshold (0.2), vertical and slope displacement, custom direction displacement, X (5 m) and Y dimension (5 m), window size interpolation (7), and dummy removal. Moreover, Fig. 5(a) showed the vertical displacement value around the study area of Palembang City from October 2014 to August 2019 which ranged from -25.2 to 10.0 cm. In general, land subsidence or negative vertical displacement occurred in the area around Palembang City.

Based on Fig. 6(a), vertical displacement in Palembang City ranged from -19.9 to 50 cm. Generally, the city experienced subsidence between -19.9 and -49,8 cm over 5 years, particularly in the northern area of Musi River (across of upstream area). The most significant subsidence area was found around Musi River, with values ranging from -30.0 to -40.0 cm. Additionally, some areas of Palembang City also experienced uplift or positive vertical displacement, ranging from 0.1 to 5 cm during the same 5-year span (2014-2019).

This uplift area was marked with a dark blue color and was relatively small in the city. In total, the subsidence phenomenon observed from August 2014 to August 2019 was included in the low vertical displacement (low deformation) category.

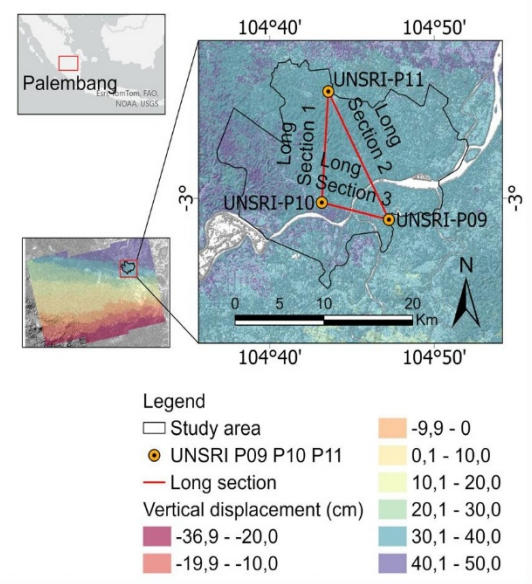

Fig. 6 Vertical displacement in August 2019 - August 2024 in Palembang City

4.3 Land Subsidence on The Longitudinal and Transverse Profile of Reference Coordinate Points

Fig. 7 showed the analysis design along the line connecting the monitoring points used to observe the elevation differences with GNSS observations reference points. This observation started from BM UNSRI-P11 point towards UNSRI-P10 covering a distance of 11.88 km. In this study, the vertical displacement value ranged from -5 cm to 1 cm along the profile. The analysis was divided into three long sections, namely long sections 1, 2, and 3. Specifically, long section 1, observed from August 2019 to August 2024, generally experienced a decrease in elevation of up to -8 cm. Long section 2 extended from BM UNSRI-P11 to BM UNSRI-P09 covering 15.26 km, and experienced a slight increase in elevation of +1 cm. The measurement points in this section were spaced 2 km apart. In total, it was observed that there was subsidence of up to -8 cm along the profile. Additionally, long section 3 covering 7.73 km from UNSRI-P10 to UNSRI-P09, showed negative vertical displacement ranging from -2 cm to -11 cm. This section typified the highest subsidence value compared to the displacement observed in long sections 1 and 2. The greatest subsidence value of -11 cm was observed 3 km from UNSRI-P10 BM point, at the intersection of the profile and Musi River. In conclusion, long section 3 experienced a significant subsidence phenomenon compared to long sections 1 and 2 over five years, since August 2019.

Upon closer inspection, the study area around Musi River was densely populated and included industrial zones located in coastal or lowland areas. These coastal areas/lowlands were formed from alluvial deposits or soil originating from river overflow due to accumulation for many years or even centuries.

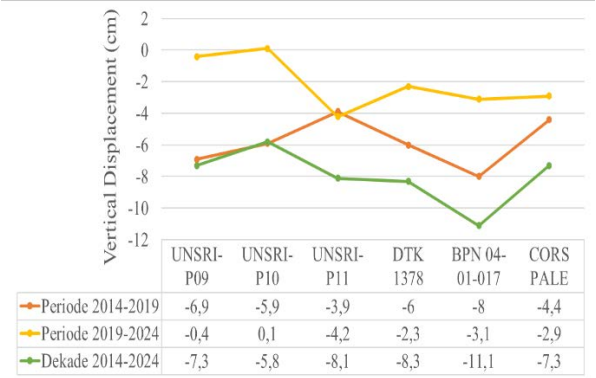

	UNSRI-P09	UNSRI-P10	UNSRI-P11	DTK 1378	BPN 04-01-017	CORS PALE
Periode 2014-2019	-6,9	-5,9	-3,9	-6	-8	-4,4
Periode 2019-2024	-0,4	0,1	-4,2	-2,3	-3,1	-2,9
Dekade 2014-2024	-7,3	-5,8	-8,1	-8,3	-11,1	-7,3

Fig. 7 Longitudinal profile (long section) of vertical displacement along the transverse profile of the installed BM UNSRI point for August 2014-2019 and 2019-2024 in Palembang City.

4.4 Land Subsidence Across The Monitoring Line At The Installed BM Point

Fig. 8 showed the area of the transverse profile, consisting of six perpendicular lines across the longitudinal profile from BM UNSRI-P10 to UNSRI-P11 with each profile spaced 2 km apart. Moreover, the distance between cross-section profiles 1 and 2 was each greater than 4 km. The areas covered by all cross-section profile lines showed both positive and negative vertical displacement, ranging from values -9 to +1 cm. In this exploration, positive vertical displacement or topographic increase occurred in the area covered by cross-section line 1, which was +1 cm for five years. Meanwhile, the area experiencing relatively high subsidence was on the cross-section profile line 6, which was -49 cm per 5 years from August 2019 to August 2024. Negative vertical displacement generally dominated the area contained by cross-sections 1 to 6, the values varying greatly.

The areas covered by each cross-section profile line experienced negative subsidence or vertical displacement with varying values ranging from -1 cm to -9 cm per five years generally in the study. Given this scenario, the area with a minimum subsidence value of -1 cm was on profile lines 1, 2, 3, and 4. Meanwhile, the area with a maximum subsidence value of -9 cm per 5 years was on around Installed BM point UNSRI-P10 to UNSRI-P09.

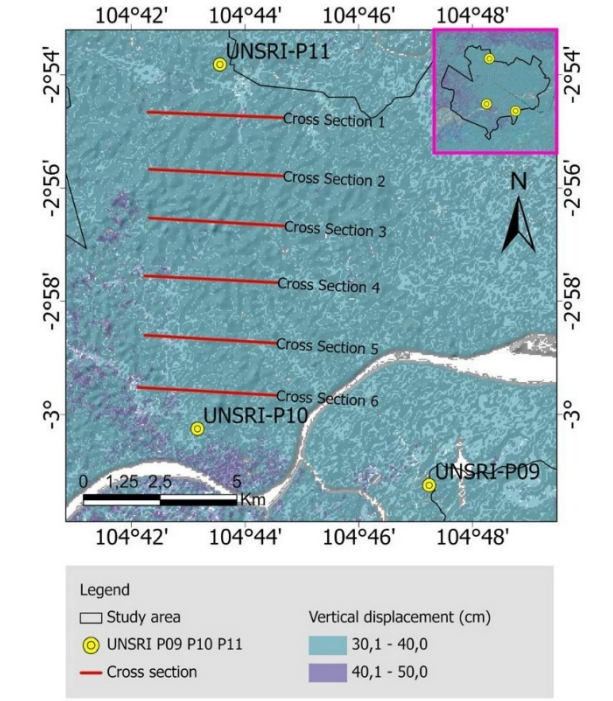

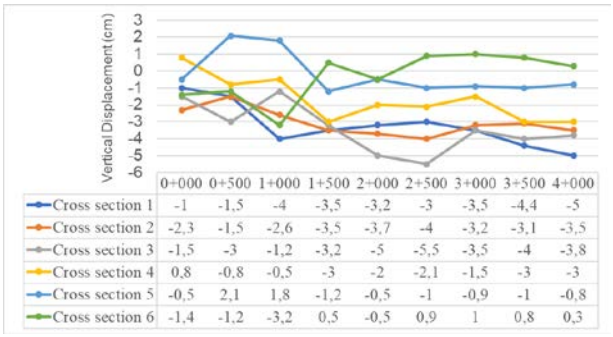

	0+000	0+500	1+000	1+500	2+000	2+500	3+000	3+500	4+000
Cross section 1	-1	-1,5	-4	-3,5	-3,2	-3	-3,5	-4,4	-5
Cross section 2	-2,3	-1,5	-2,6	-3,5	-3,7	-4	-3,2	-3,1	-3,5
Cross section 3	-1,5	-3	-1,2	-3,2	-5	-5,5	-3,5	-4	-3,8
Cross section 4	0,8	-0,8	-0,5	-3	-2	-2,1	-1,5	-3	-3
Cross section 5	-0,5	2,1	1,8	-1,2	-0,5	-1	-0,9	-1	-0,8
Cross section 6	-1,4	-1,2	-3,2	0,5	-0,5	0,9	1	0,8	0,3

Fig. 8 Cross-section profile of vertical displacement around Installed BM point UNSRI-P11 to UNSRI-P10, August 2019 – August 2024 period

4.5 Correlation of Land Subsidence To The Geological Conditions of Palembang City

When viewed from the aspect of rock structure, Palembang City area was generally formed from surface sedimentary rock structures, Miocene sedimentary rocks (early, middle, and late), Oligocene (late), and Halocene sedimentary rocks. In Fig. 10, the surface sedimentary rock structure, namely Swamp Deposits (Qs) dominated the city area at around 77.65%, with a distribution area starting from the northern area to the west. Airbenakat Formation covered about 20% of the area, extending from the west to the north with a thickness ranging from 1,000-1,500 m. Meanwhile, Gumai Formation covered around 0.55% with a varying thickness reaching up to 2,700 m and Talangakar Formation covered about 0.09% of the area with a thickness of around 610 m.

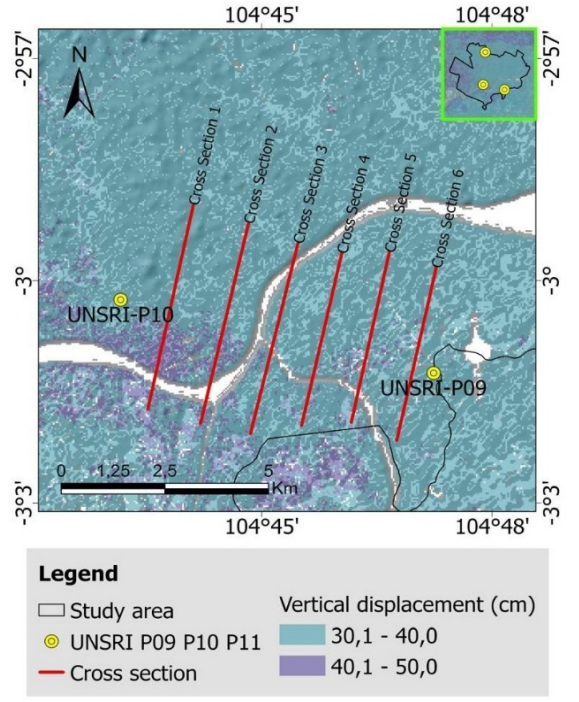

	0+000	0+500	1+000	1+500	2+000	2+500	3+000	3+500	4+000
Cross section 1	2,5	0,7	4	3	2,2	0,2	0,6	0,1	0,8
Cross section 2	4	1	3,5	0,8	2,5	2	1,2	0,5	0,1
Cross section 3	4	2,2	2	2	2,1	1	0,4	1,8	-1
Cross section 4	1,5	1	1	0,9	-0,2	-0,3	-0,4	-0,8	-0,7
Cross section 5	-1,8	-2	-2	1	0,5	-1	0,8	-0,4	0,2
Cross section 6	-0,2	0,5	0,4	-0,4	0,7	-2,5	-0,3	0,7	0,2

Fig. 9 Cross-section profile of vertical displacement around Installed BM point UNSRI-P10 to UNSRI-P09, August 2019-August 2024 period

Relating to the discussion, Gumai Formation and Talang Akar Formation spread to the northwest of Palembang City.

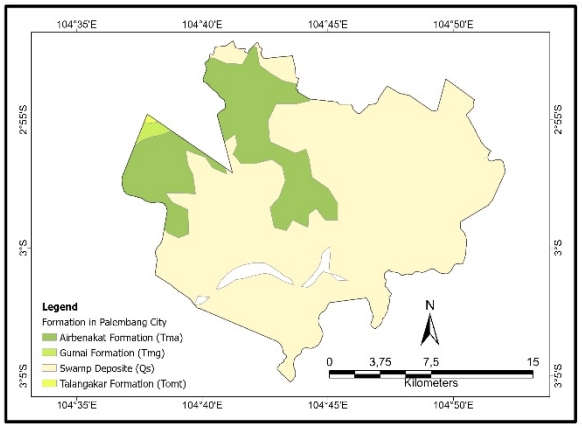

Fig. 10 Stratigraphic distribution of geological formations in Palembang City

In comparison with land subsidence in other Indonesian cities, such as Jakarta (- 3 to - 10) Cm/year, Semarang (-6 to -8) Cm/year, Surabaya (-6 to -10) Cm/year, and Bandung (- 7.6 to – 23) cm/year, Palembang City was significant enough to be considered in reducing the rate of land subsidence, by paying adopting more adaptive spatial development patterns. During spatial development planning for Palembang City, a critical consideration was minimizing the filling of swamps for the construction of residential infrastructure and other city facilities. Since the potential for subsidence on embankment land was very high, a building permit (IMB) would be required with better consideration in low areas with elevations < 5 m msl. Additionally, special conditions needed to be implemented with more adequate considerations, particularly regarding the structure of the building foundation.

5. CONCLUSION

In conclusion, the following observations were made from this study.

1. The subsidence observed in Palembang City area was attributed to urban development, particularly the expansion of infrastructure. Changes in the total floor area of buildings contributed to the acceleration of land subsidence.
2. Factors of multi-story building structures and the distance between buildings affected the varying superimposition effects of subsidence, specifically in the central urban area, which was characterized by an increase in multi-story buildings on a large scale.
3. In the period from October 2019 to August 2024, Palembang City experienced subsidence ranging from -19.9 to -49.9 cm for five years, which was found in the northern area of Musi River (across downstream area). Moreover, the highest subsidence area was located in the area around Musi River, ranging from -30 to -50.0 cm for Oct 2023 to Oct.2024
4. Palembang City area experienced positive vertical uplift or displacement, which ranged from 0.1 to 5 cm for five years, from October 2014 to August 2019.
5. During the last 4 years, from August 2019 to August 2024, the northern part of the city, namely across downstream area, experienced subsidence of -19.6 to -51.9 cm. And this decline is higher than the land subsidence that occurred in other cities in Indonesia.
6. Palembang City was significant enough to be considered in reducing the rate of land subsidence, by paying attention to more adaptive spatial development patterns.

6. ACKNOWLEDGMENTS

The authors are grateful to the Directorate of Research Technology and Community Service, Directorate General of Higher Education, Research and Technology, Ministry of Education, Culture, Research and Technology, the Republic of Indonesia, who has provided research funding through Doctoral Research grants based on Master Contract No.:090/E5/PG.02.00.PL/2024, Date : June 11, 2024 and Derivative contrats No. 0016.003/UN9/ SB1.LP2M.PT/2024, Date June 19, 2024.

7. REFERENCES

[1] Julzarika A., Aditya T., Subaryono S and Harintaka H., Dynamics Topography Monitoring in Peatland Using the Latest Digital Terrain Model, Journal Application Engineering. Sci., vol. 20, no. 1, pp. 246–253, 2022, doi: 10.5937/jaes0-31522.

[2] Ramirez R., Abdullah R.E., Jang Y., Choi S.K., Kwon T.H., Satellite-based monitoring of an open-pit mining site using Sentinel-1 advanced radar interferometry: a case study of the December 21, 2020, landslide in Toledo City, Philippines, E3S Web of Conferences 415,05020, Vol. 415, 2023, pp. 1-4. https://doi.org/10.1051/ e3sconf/202341505020.

[3] Gumilar I., Sidiq T.P., Virtriana R., Pambudi G., Bramanto B., Abidin H.Z., Geodetic Observations Confirming Land Subsidence of Bandung Basin, Indonesia and Subsequent Building Damage, Acta Geodaetica et Geophysica, July, 2023, Volume 58, pp. 373-388.

[4] Cigna F., Tapete D., Monroy G.V.H., Muñiz-Jauregui J.A., Hernández G.O.H., and Haro J.A., Wide-area InSAR survey of surface deformation in urban areas and geothermal fields in the eastern Trans-Mexican Volcanic Belt, Mexico, Remote Sensing, vol. 11, no. 20, 2019. pp. 1–33, doi: 10.3390/rs11202341.

[5] Castellazzi P., Garfias J., and Martel T., Assessing the efficiency of mitigation measures to reduce groundwater depletion and related land subsidence in Querétaro (Central Mexico) from decadal InSAR observations, International Journal Application Earth Observation Geoinf., vol. 105, no. November, 2021. p. 102632, doi: 10.1016/j.jag.2021.102632.

[6] Ramirez R.A., Abdullah R.E.E and Rubio C.J.P, S1-PSINSAR Monitoring and Hyperbolic Modeling of Nonlinier Ground Subsidence in Naga City, Cebu Island in The Philippines, International Journal of GEOMATE, Dec, 2022, Vol.23, Issue 100, pp.102-109. DOI: https://doi.org/10.21660/2022.100.g12121

[7] Rosidi M.S., Prastama R.A., Yusuf M.,Daud Y., Monitoring of Jakarta Subsidence Applying 4D Microgravity Survey Between 2014 and 2018, International Journal of GEOMATE, March., 2021, Vol.20, Issue 79, pp. 132-138. DOI: https://doi.org/10.21660/2021.79.j2031

[8] Bott L.M., Schöne T., Illigner J., Haghshenas Haghighi M., Gisevius K and Braun B., Land Subsidence in Jakarta and Semarang Bay – The relationship between physical processes, risk perception, and household adaptation, Ocean Coast Management, Vol. 211, 2021, doi: 10.1016/j.ocecoaman.2021.105775.

[9] Andriani, Harliz A., Hadie M.S.S.N., Putra H.G., Ibrahim E., Putranto D.D.A., Khaliq A., Multicriteria analysis of factors causing land subsidence at lowlands area (case study at Tanjung Api-Api Area), AIP Conference Proceeding, Vol. 3026, 080037, Issue 1, March 18, 2024, pp. 1–7, doi: https://doi.org/10.1063/5.0199749.

[10] Ramirez R.A., Abdullah R.E.E and Rubio C.J.P., Satellite-Based Ground Deformation Monitoring in Naga City, Cebu Island in The Phiippines, Procceding, 12th Int. Conf. on Geotechnique, Construction Materials & Environment, November 2022, pp. 41–46.

[11] Xiong J., Xiao R, and He X, Land Surface Deformation in Nanchang, China 2018–2020 revealed by multi-temporal InSAR, Nat. Hazards Res., Vol. 1, no. 4, 2021, pp. 187–195. doi: 10.1016/j.nhres.2021.10.003.

[12] Wiharso D., Affandi, Cahyono P., Loekito S., Nishimura N., Senge M., Effect of Long-Term Cassava Cultivation on The Morphology and Properties of Soils in Lampung, Southern Sumatera, Indonesia, International Journal of Geomate, March., 2021, Vol.20, Issue 79, pp. 168-176. DOI: https://doi.org/10.21660/2021.79.j2053

[13] Sowter A., Bin M, Amat C., Cigna F., Marsh S., and Athab A., Mexico City Land Subsidence in 2014 – 2015 with Sentinel-1 IW TOPS : Results using the Intermittent SBAS (ISBAS) technique, International Journal Application Earth Observation Geoinformation., Vol. 52, pp. 230–242, 2016, doi: 10.1016/j.jag.2016.06.015.

[14] Haghighi M.H., and Motagh M., Sentinel-1 InSAR over Germany : Large-Scale Interferometry, Atmospheric Effects, and Ground Deformation Mapping, Vol. 4, 2017. pp. 245–256. doi: 10.12902/zfv-0174-2017.

[15] Ardha M., Suhadha A.G.1., Julzarika1 A., Yulianto F., Yudhatama D., and Darwista R.Z., Utilization of Sentinel-1 satellite imagery data to support land subsidence analysis in DKI Jakarta, Indonesia, Journal Degradation Mineral Land Management., Vol. 8, 2021. ISSN: 2339-076X (p); 2502-2458 (e), pp. 2587–2593. doi: 10.15243/jdmlm.

[16] Sabri L.M., Vertical Reference System in Land Subsidence Areas, Disertation, UGM, 2018. pp. 1-278

[17] ESA, Sentinel Satellites. European Space Agency,2019.https://www.esa.int/OurActivities /Observing the_Earth/Copernicus/Overview4.

[18] Constán R.A., Armenteros R.A.M., Fernández L.F., Rosillo M.S., Delgado J. M., Bekaert D. P. S., Sousa J.J., Gil, A.J., Cuenca C.M., Hanssen R. F., Zaldívar G.J., and Galdeano S.C., Multi-temporal InSAR evidence of ground subsidence induced by groundwater withdrawal: the Montellano aquifer (SW Spain). Environmental Earth Sciences, 75(3),2016.pp1–16. https://doi.org/10.1007/s12665-015-5051-x

[19] Constán R.A., Armenteros R.A.M., Rosillo M.S., Zaldívar G.J., Lazecky, M., García, M., Sousa J.J., Galdeano S.C., Blasco D.J.M., Gavilán J.P., Cuenca C.M., Espinar L.J.A., SAR interferometry monitoring of subsidence in a detritic basin related to water depletion in the underlying confined carbonate aquifer (Torremolinos, southern Spain), Science of the Total Environment, No. 636, 2018, pp. 670–687. https://doi.org/10.1016/j.scitotenv.2018.04.280

[20] Du Z., Ge L. Ng A.H.M., Zhu Q., Yang X., Li L., Correlating the subsidence pattern and land use in Bandung, Indonesia with both Sentinel-1/2 and ALOS-2 satellite images. International Journal of Applied Earth Observation and Geoinformation, Vol. 67, January, 2018, 54–68. https://doi.org/10.1016/j.jag.2018.01.001

[21] Julzarika A., DTM update model using Alos Palsar/Palsar-2 and Sentinel-1 imagery for dynamic topography, Disertation,UGM, 2021, pp 1-151.

[22] Ferretti A., Prati C., Rocca F., and Guarnieri M.A, Guidelines for SAR Interferometry Processing and Interpretation. In InSAR Principles, 2017.

[23] Onačillová K.,Gallay M., Paluba D., Péliová A., Tokarčík O., and Laubertová D., Combining Landsat 8 and Sentinel-2 Data in Google Earth Engine to Derive Higher Resolution Land Surface Temperature Maps in Urban Environment, Remote Sensing, vol. 14, no. 16, 2022, p. 4076. doi: 10.3390/rs14164076.

[24] Chini M., Pelich R., Pulvirenti L., Pierdicca N., Hostache R., and Matgen P., Sentinel-1 InSAR Coherence to Detect Floodwater in Urban Areas : Houston and Hurricane Harvey as A Test Case, 2019, pp. 1–20, doi: 10.3390/rs11020107.